Reaction Pathways of GaN (0001) Growth from Trimethylgallium and Ammonia versus Triethylgallium and Hydrazine Using First Principle Calculations

ARTICLE *in* THE JOURNAL OF PHYSICAL CHEMISTRY C · FEBRUARY 2015

Impact Factor: 4.77 · DOI: 10.1021/jp5116405

1 AUTHOR:

Andres Jaramillo-Botero
California Institute of Technology
45 PUBLICATIONS **210** CITATIONS

SEE PROFILE

THE JOURNAL OF PHYSICAL CHEMISTRY C

Article

pubs.acs.org/JPCC

Reaction Pathways of GaN (0001) Growth from Trimethylgallium and Ammonia versus Triethylgallium and Hydrazine Using First Principle Calculations

Qi An,[†] Andres Jaramillo-Botero,*[,†] Wei-Guang Liu,[†] and William. A. Goddard, III*[,†]

[†]California Institute of Technology, Pasadena, California 91125, United States

ABSTRACT: Gallium nitride (GaN) is a wide bandgap semiconductor with many important applications in optoelectronics, photonics, and both high power and high temperature operation devices. Understanding the surface deposition mechanisms and energetics for different precursors is essential to improving thin-film crystalline quality and growth process requirements for extended engineering applications. Here, we use ab initio calculations to study the reaction mechanisms of GaN thin film growth on (0001) surface from ammonia (NH_3) and hydrazine (N_2H_4), nitrogen precursors, and trimethylgallium (TMG) and triethylgallium (TEG), gallium precursors. We find that the initial dehydrogenation of N_2H_4 is more facile than that of NH_3, at 1.15 versus 13.61 kcal/mol, respectively, and that neighboring adsorbed surface hydrogens reduce the barriers for further decomposition of NH_2 and NH. We also find that the growth of nitrogen layers is a reaction-limited process rather than diffusion-limited at low adsorbate coverage. On the other hand, the deposition of Ga on a nitrogen rich surface via TMG is limited by the abstraction reaction of the second methyl (CH_3) group in TMG, with a barrier of 42.54 kcal/mol. The mechanisms of adsorption of TMG and TEG are different, whereas TMG dissociatively chemisorbs releasing one methane group, the beta-hydrate elimination (C_2H_4 + H) in TEG is favored through surface interactions (without chemisorption) at a comparable energy barrier to the first CH_3 dissociation in TMG. This does not suggest a more favorable thermodynamic route to low-temperature growth, but it does favor TEG for avoiding the explicit abstraction or insertion of C groups during metalorganic chemical vapor deposition (MOCVD) or atomic layer deposition (ALD) techniques.

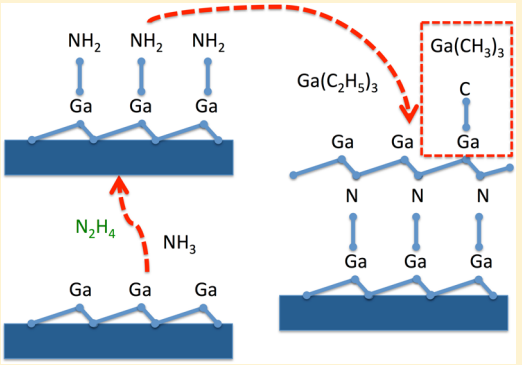

I. INTRODUCTION

Gallium nitride (GaN) is a wide band gap material (direct band gap of 3.4 eV), with high breakdown field, high thermal and chemical stability, and high saturation drift velocity.[1−10] The combination of these properties makes it an ideal material for extended use in light emitting diodes (LEDs), laser diodes (LDs), photonics and high-power and high-temperature operation devices.[1−11] However, extended applications have been hindered by the challenges involved in producing high-quality crystalline films due to the significant lattice mismatches when growing on common substrates such as sapphire, GaAs and SiC.[12,13] Albeit the use of buffer layers has minimized the lattice mismatch effects (e.g., AlN), improved quality, epitaxially grown GaN films requires full understanding of the growth parameters and mechanisms.[14−16] Despite numerous experimental and theoretical studies, the GaN growth mechanisms remain controversial because of the complex surface reactions (particularly through the nonadduct route shown in Figure 1).

GaN thin films can be synthesized experimentally through various methods including metal−organic vapor phase epitaxy (MOVPE),[17] molecular beam epitaxy (MBE),[18] sputtering processes,[19] and supersonic gas jet assisted vapor deposition.[20,21] The quality of GaN films depend significantly on the deposition method. MOVPE is known to grow the best quality of GaN to date. However, this process requires very high temperatures (1000 °C) to dissociate nitrogen from its precursor, typically NH_3.[6] As a consequence of the high temperature significant lattice mismatch occurs between the substrate and the grown film, because of a significant difference in the thermal expansion coefficients.[6] This also leads to other undesired effects such as metal desorption, diffusion, and segregation.[6] Thus, it is desirable to reduce the GaN growth temperature to produce high quality thin film for engineering applications. However, most experiments[22,23] have found that the growth of GaN thin films at low temperature (<500 °C) leads to unwanted amorphous phases and that crystallinity improves as the deposition temperature increases.

Computational fluid dynamics and kinetic Monte Carlo simulation methods have been used to steer the design, optimization, and troubleshooting of GaN growth processes.[24,25] However, the efficacy of such models is limited by the availability of accurate kinetics information, particularly associated with the chemical reaction mechanisms and energetics of growth as a function of temperature. Density

Received: November 20, 2014
Revised: January 18, 2015

DOI: 10.1021/jp5116405
J. Phys. Chem. C XXXX, XXX, XXX−XXX

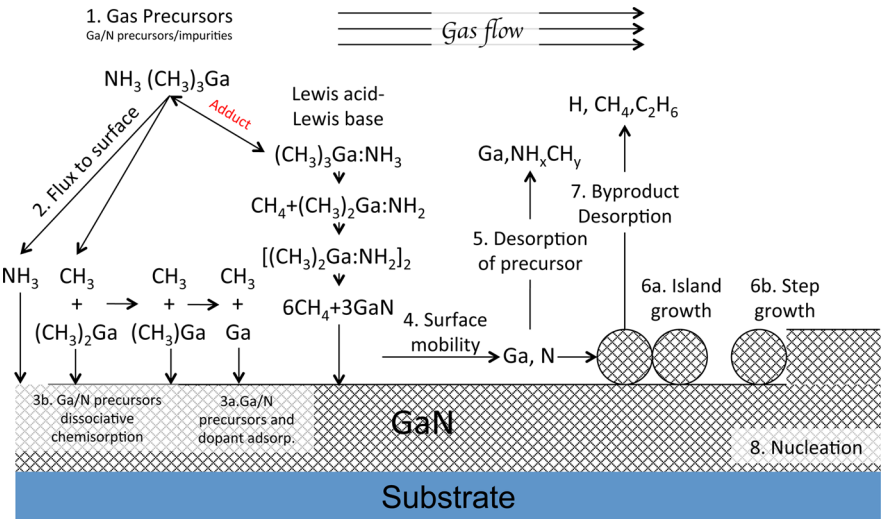

Figure 1. Gallium nitride growth pathways (flux, surface chemistry, surface mobility, byproduct removal, and growth) from trimethylgallium and ammonia.

functional theory (DFT) calculations have also been widely used to examine GaN surface models. In particular, the GaN (0001) surface and its coverage with H and N atoms has been extensively studied.[26−34] The gas phase and surface reactions using ammonia (NH_3) and trimethylgallium (TMG) as precursors have also been studied using ab initio finite cluster simulations.[1,35−37] The gas phase reactions are well summarized and documented in previous studies.[1] However, a complete study of the surface reaction mechanisms, including chemisorption of reactive species from the gas-phase, decomposition and recombination reactions on the surface, and thin film growth reactions (see Figure 1) is absent due to the large number of gas-phase species that can adsorb onto the surface under different experimental conditions.[1]

In this paper, we use first-principles quantum mechanics (DFT) to examine the GaN (0001) surface chemical reactions using different precursors, namely, ammonia (NH_3) and hydrazine (N_2H_4) nitrogen sources, and trimethylgallium (TMG) and triethylgallium (TEG) gallium sources. The binding energies for NH_3, N_2H_4 and the corresponding decomposed species are calculated, as well as the transition pathways for the decomposition reactions, hydrogen transfer events that facilitate the decomposition reactions, and the diffusion barriers for surface migration of the decomposed species. We examine the TMG surface reactions mechanism on an N-rich surface, and we compare it with the beta-hydrate elimination reactions of TEG in the gas phase. Our results provide important clues into the mechanisms of GaN thin film growth and points out the key steps that need to be addressed for low substrate temperature growth.

II. COMPUTATIONAL METHODS

For periodic calculation, we applied the Perdew−Burke−Ernzerhof (PBE) exchange−correlation functional implemented in the VASP package,[38−40] using the projector-augmented wave method[41] to account for the core−valence interactions. We focused on the GaN (0001) polar surface. The Ga 3d electrons are treated as core electrons. To examine the surface reactions of NH_3 and N_2H_4, we used a periodic slab of five double layers of GaN, 15 Å of vacuum between the slabs, and a (2 × 2) surface unit cell. A (3 × 3 × 1) Monkhorst−Pack grid for k-point sampling was used for this surface model. To simulate the TMG surface reaction, we rotated the unit cell to make "a" along $(2\bar{1}\bar{3}0)$ direction and "b" along $(01\bar{1}0)$ direction. Then we made a (2 × 2) rotated cell with four double layers along (0001) direction. Here, we define the double layer as one Ga−N layer of thickness half c-lattice constant. This corresponds to eight Ga atoms for each double layer. Only the gamma point was sampled in the Brillouin zone for this model. The atoms in the bottom layer were passivated with fractionally charged (0.75e) H atoms. Only the top two double layers were allowed to relax. Relaxation of the third double layer leads to an energy difference that is less than 0.001 eV with respect to the system with only the top two layers relaxed, and hence, the latter was chosen as an accurate and computationally efficient model. We used a kinetic energy cutoff of 400 eV for the plane wave expansions in periodic calculations. The convergence criteria were set to a 1×10^{-5} eV energy difference for solving the electronic wave function and a 1×10^{-2} eV/Å force for geometry optimization. Dipole corrections and surface spin-polarization were allowed in all calculations because of the experimentally observed polar nature of the GaN(0001) surface. Spin polarization is needed to account for possible changes in spin state as reactions occur on the surface.

To examine the beta hydride elimination reaction, we carried out finite cluster QM calculations in Jaguar[42] using the PBE functional and lacv3p++ G(d,p) basis set. We used the PBE functional to allow direct comparisons with the periodic calculations. The transition states were validated to have exactly one negative eigenvalue of the Hessian. We then followed the minimum energy path to identify and connect reactants and products.

To identify transition states and to calculate activation barriers in the periodic slab model for N_2H_4, NH_3 decomposition reactions as well as N_xH_y (x = 0,1; y = 0−3) diffusion, we used the climbing image nudged elastic band method (CINEB)[43] with five intermediate images between the reactions' initial and final states. To examine the TMG reaction transition state and reaction barrier on the N-rich surface, we used the dimer transition state search method.[44] The obtained transition states were verified by vibrational analysis that confirm only one imaginary frequency. The dynamical matrix

DOI: 10.1021/jp5116405
J. Phys. Chem. C XXXX, XXX, XXX−XXX

was determined by displacing each ion of 0.15 Å in the direction of each Cartesian coordinate and from the corresponding forces. Only the top two layers are relaxed in the vibrational analysis, without loss of chemical accuracy.

III. RESULTS AND DISCUSSION

III-1. Nitrogen Species on GaN (0001) Surface. *III-1-1. Bare GaN (0001) Surface Model.* We first examine the chemical reactions of nitrogen precursors (NH_3 and N_2H_4) on a bare Ga surface where the Ga dangling bonds are partially filled with 3/4 electrons. GaN (0001) surface reconstruction had been widely examined experimentally and computationally.[26−30] We started with a (2 × 2) bare Ga surface, as shown in Figure 2a, and displaced half the surface Ga atoms

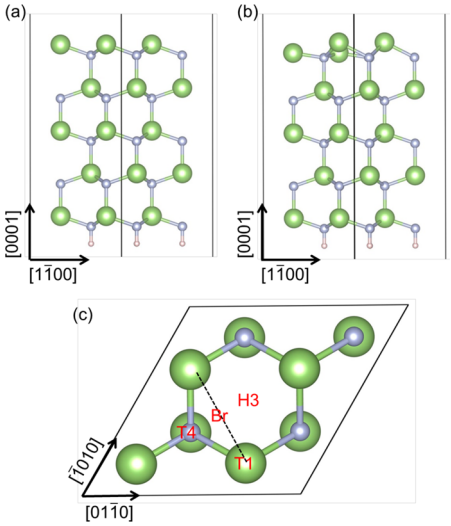

Figure 2. Simulation model of GaN (0001) surface: (a) side view for the no reconstruct surface; (b) side view for the reconstruct surface; (c) the top view. The Ga, N, and H atoms are shown by green, gray, and white balls, respectively.

downward. This structure was minimized to obtain a reconstructed surface, as shown in Figure 2b. The reconstructed surface is 0.13 J/m^2 lower in energy than the unreconstructed surface. For the reconstructed surface, half of the Ga atoms move inward and below the N layers and form sp^2 type bonds in a nearly planar structure with three nitrogen atoms. However, the other half of Ga atoms remain in the tetrahedral bonding formation, as the unconstructed surface. Although there is no current experimental evidence, previous DFT studies found similar GaN (0001) surface reconstruction, where the surface energy is ∼12−16 J/m2 lower in total energy.[45,46] This surface reconstruction is also similar to those in previously reported QM studies on InN (0001) surface.[47]

III-1-2. N_xH_y (x = 1,2; y = 0−4) Binding Energy. Binding energies of NH_3 and N_2H_4 species and their fragments on GaN (0001) surface were computed as

$$E_{bind} = E_{sur-mol} - E_{surf} - E_{g\,mol} \quad (1)$$

where $E_{sur\text{-}mol}$ corresponds to the total energy of molecular species on the surface, E_{surf} is the total energy of the reconstructed surface, and $E_{g\,mol}$ is the energy of the corresponding molecules in gas phase. A negative value of E_{bind} indicates an exothermic process. Table 1 lists the binding energies of N_2H_4, NH_3, NH_2, NH, N, and H at 0.25 ML coverage at the various binding sites indicated in Figure 2c.

Table 1. Binding Energy (Unit: kcal/mol) of $N_{x\,=1,2}H_{y\,=\,0\text{-}4}$ Species on the Pure Ga Surface

species	T1	T4	H3	Br
N_2H_4	−33.44	...	...	−38.05
NH_3	−32.75	...	...	...
NH_2	−84.17	...	...	−89.70
NH	...	−114.15	−129.83	...
N	...	−109.99	−127.29	...
H	−75.18	...	...	...

NH_3 was only found to be stable at the top (T1) site with an E_{bind} of −32.75 kcal/mol, which is stronger than NH_3 bonded to InN surface of −20.06 kcal/mol.[47] The resulting Ga−N and N−H bond lengths are 2.10 and 1.03 Å, respectively, and the H−N−H angles are 108.6°, 108.7°, and 111.2°.

In contrast, N_2H_4 was found to be stable at T1 and bridge (Br) sites, with an E_{bind} of −33.24 kcal/mol and −38.05 kcal/mol, respectively. On the T1 site, one of N atom in N_2H_4 is bonded to surface Ga with the Ga−N bond length of 2.11 Å. The N−N bond tilted upward with a Ga−N−N angle of 112.3° and a N−N bond length of 1.44 Å, which coincides with the single N−N bond length. For the Br site, the N−N bond is parallel to the Ga surface and two N atoms are bonded to two surface Ga atoms. In this geometry, the Ga−N and N−N bond lengths are 2.33 and 1.46 Å, respectively. The corresponding N−H bond lengths are 1.03, 1.05, and 1.06 Å. The H−N−H angle is 110.0°, which is slightly larger than that of a gas phase system (107.2°). The H−N−N−H torsion angles are 47.1° and 72.6°, compared with the corresponding gas phase angles of 30.4° and 87.2°. N_2H_4 bound on a Br site is shown in Figure 3d.

NH_2 binds stably to T1 and Br sites, with binding energies of −84.17 kcal/mol and −89.70 kcal/mol, respectively. In the T1 configuration, the N of the NH_2 molecule is 1.90 Å away from the surface Ga. The N−H bond lengths are 1.02 Å and the H−N−H angle is 109.7°, which differs slightly from the gas phase values of 1.04 Å and 102.1°. In the bridging configuration, NH_2 is adsorbed between two Ga atoms with the two H atoms pointing upward. The N−H and Ga−N bond lengths in this configuration are 1.03 and 2.13 Å, respectively, and the H−N−H angle is 108.0°. The Br site is energetically more stable by 5.53 kcal/mol than the T1 site.

For NH, the hollow (H3) site was found to be energetically most favorable with a binding energy of −129.83 kcal/mol. In this configuration, N forms three bonds with the surrounding Ga atoms with a Ga−N bond length of 2.10 Å and an N−H bond length of 1.03 Å, which is slightly shorter than the gas phase value of 1.05 Å. The T4 site was found to be energetically least favorable by 15.68 kcal/mol due to the steric repulsion from subsurface N.

N binding is energetically more favorable on the H3 site, with a binding energy of −127.29 kcal/mol. In this geometry, the Ga−N bond length is 2.03 Å.

Finally, the only stable adsorption site for H atoms was found to be the T1 sites, with a binding energy of −75.18 kcal/mol referenced to hydrogen atom. In this geometry, the Ga−H bond length is 1.58 Å.

We find that the adsorption energies for N_xH_y (x = 0,1; y = 0−3) becomes more negative as the number of H atoms

DOI: 10.1021/jp5116405
J. Phys. Chem. C XXXX, XXX, XXX−XXX

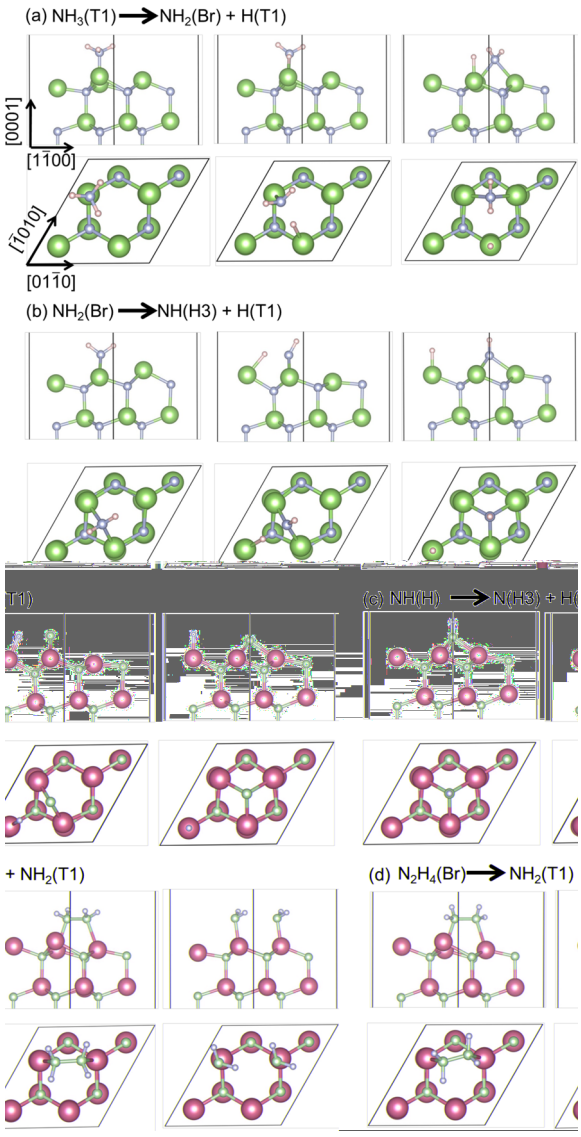

Figure 3. NH_3 and N_2H_4 dehydrogenation reaction mechanism on Ga (0001) surface. The initial (left), transition (center), and the product (right) states are viewed from side and top. The Ga, N, and H atoms are represented by green, gray, and white balls, respectively.

decreases. Also, the distance from the N atoms to the surface Ga atoms decreases with a smaller number of H atoms in the molecule, indicating a stronger interaction of the dehydrogenated species with the surface. The N and NH species have the lowest surface binding energy on H3 site, which is consistent with recent experimental observations that the 2 × 2 surface reconstruction after growth under N-rich conditions is associated with N adatoms in the H3 configuration.[48] The binding energy of N_2H_4 on Br sites is more negative (by 5.3 kcal/mol) than NH_3 on T1 sites, indicating that the N_2H_4 will adsorb easier into the Ga surface than NH_3. Therefore, we confirm that N_2H_4 leads to higher N yield than NH_3 for GaN thin film growth, which is consistent with experimental observation that GaN growth could happen at significant lower temperature using N_2H_4 as N source than using NH_3,[49] and we contend that it enables a lower growth temperature by virtue of the larger binding energy than ammonia.

III-1-3. NH_3 and N_2H_4 Decomposition Reactions on the GaN (0001) Surface. To confirm which is the better nitrogen precursor for the GaN thin film growth, we examined the N_2H_4 and NH_3 decomposition reactions on the GaN (0001) surface. We first study the NH_3 decomposition reactions starting from a stable T1 site. The geometries of initial, final, and transition states are shown in Figure 3a, and the reaction barriers and heat of reactions are listed in Table 2. We find that the NH_3 is decomposed to one H on the T1 site and one NH_2 on the bridge site with the reaction barrier of 13.61 kcal/mol. At the transition state, the NH_3 molecule is pushed to the Br site and the N−H bond stretches from 1.04 to1.48 Å. This is an exothermic reaction releasing 16.37 kcal/mol of energy. Subsequently, the NH_2 is decomposed to NH on a H3 site and H on a T1 site with a reaction barrier of 21.68 kcal/mol (Figure 3b). At the transition state, the N−H bond is stretched to 1.58 Å. This is also an exothermic reaction that releases 14.99 kcal/mol in energy. Finally, the NH is decomposed to one N on an H3 site and an H on a T1 site (Figure 3c). This reaction has a high barrier, 70.79 kcal/mol, and corresponds to an endothermic process that absorbs 36.90 kcal/mol in energy.

Table 2. N_2H_4 and NH_3 Surface Decomposition Reactions (Unit: kcal/mol) on the Ga Surface[a]

reactions	reaction barrier	heat of reaction
NH_3(T1)=>NH_2(Br) + H(T1)	13.61	−16.37
NH_2(Br)=>NH(H3) + H(T1)	21.68	−14.99
NH(H3)=>N(H3) + H(T1)	70.79	36.90
N_2H_4(Br)=>2NH_2(T1)	1.15	−50.96
NH_2(T1) + NH_2(Br)=>NH_3(T1) + NH(H3)	13.61	11.07
NH_2(T1) + NH(H3)=>NH_3(T1) + N(H3)	36.67	27.44
NH(H3) + NH(H3)=>NH_2(T1) + N(H3)	22.83	2.31

[a]The first four reactions correspond to the reactions described in Figure 3 in sequence, and the last three reactions correspond to the reactions described in Figure 4 in sequence.

We then examined the N_2H_4 decomposition reaction starting from the most stable Br site. The initial, final, and transition state geometries are shown in Figure 3d. At the transition state, the N−N bond rotates to align along the Ga−Ga bond before bond breaking. Then, N_2H_4 decomposes in two NH_2 on the T1 sites with a reaction barrier of 1.15 kca/mol, releasing 50.96 kcal/mol of energy. The small decomposition reaction barrier confirms that the N_2H_4 decomposes readily on the GaN (0001) surface, and the much larger 50.96 kcal/mol energy release, compared to NH_3 decomposition, indicates it is a better precursor for low-temperature growth of GaN. The very low barrier of hydrazine decomposition is due to its N lone pair interacting with and bonding with the empty orbital of a surface Ga. This is consistent with the previous DFT study of the hydrazine decomposition on Rh (111) and Ir(111) surface, where its N−N bond strength is dramatically decreased when compared to the gas phase molecule.[50,51]

The large kinetic barriers for NH_2 and NH decomposition reactions as discussed above imply that the formation of active N species may limit the growth process. However, we find that the presence of neighboring NH_2 and NH species lowers the corresponding reaction barriers through hydrogen transfer. Figure 4 shows the initial, final, and transition state geometries of hydrogen transfer reactions. The calculated reaction barriers and heat of reactions are summarized in Table 2. In the first reaction (Figure 4a), H is transferred from one NH_2 on a Br site to a neighboring T1 site to yield NH at the H3 site and

DOI: 10.1021/jp5116405
J. Phys. Chem. C XXXX, XXX, XXX−XXX

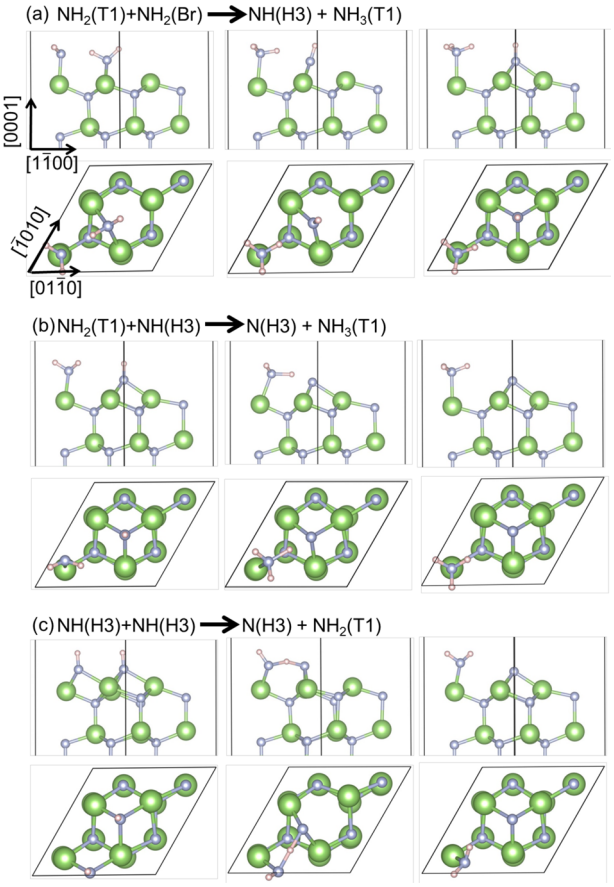

Figure 4. Side and top views of the initial (left), transition (center), and the final (right) states for reactions involving H transfer between adsorbed molecules on the GaN (0001) surface. Green, gray, and white balls represent the Ga, N, and H atoms, respectively.

NH_3 at the T1 site. The barrier for this reaction is 13.61 kcal/mol, which is 8.07 kcal/mol lower than the barrier for NH_2 decomposition by hydrogen dissociation. Active N species, on the other hand, can be produced in reactions between NH and NH_2 at H3 and T1 sites, respectively, or two NH molecules at H3. The barriers for these processes are 36.67 and 22.83 kcal/mol, respectively, which are significantly lower than the barrier for the NH dissociation process. If N_2H_4 is used as the nitrogen precursor, it not only decomposes into two NH_2 to improve the N yield, compared to NH_3, but it could also provide the H transfer source to facilitate the decomposition reactions. Thus, we contend that N_2H_4 is a better and more amenable to low-temperature growth nitrogen precursor than NH_3.

III-1-4. Nitrogen Species Surface Diffusion. To check how the diffusion of species affects the GaN growth process, we calculated diffusion barriers for NH_3, NH_2, NH, N, and H between their stable sites (as listed in Table 3). From surface chemistry experiments and first-principles calculations, we conclude that reactions with energy barriers of up to 15 kcal/mol can proceed below 100 °C. We find that NH and NH_2 mobility will occur on substrate temperatures below 100 °C with the maximum barrier of 17.53 from H3 site to T4 site, which allows for the H transfer reactions to take place. N atoms diffusing from an H3 site to a T4 site, with an energy barrier of 27.9 kcal/mol, will require temperatures in the order of 150°-200 °C. as well as NH_3 and H mobility from a T1 site to a T1 site (21.45 and 20.98 kcal/mol, respectively). Overall, the

Table 3. Decomposed Species and NH_3 Diffusion Barriers (Unit: kcal/mol) on the Ga Surface[a]

N species	diffusion barrier
NH_3 (T1=>T1)	21.45
NH_2 (T1=>Br)	0.69
NH_2 (Br=>T1)	6.23
NH_2 (Br=>Br)	9.69
NH (H3=>T4)	17.53
NH (T4=>H3)	1.84
N (H3=>T4)	27.90
N (T4=>H3)	10.84
H (T1=>T1)	20.98

[a]The terms in parentheses correspond to the diffusion paths defined in Figure 2.

relatively low diffusion barriers indicate that the N layer growth process is primarily a reaction-limited process as opposed to a diffusion-limited process under low surface coverage conditions.

III-1-5. Discussion on Nitrogen Growth Process. Our current simulations focus on the bare Ga surface. Previous studies constructed the phase diagram of GaN (0001) surface in an ammonia environment and based on the chemical potential of hydrogen and nitrogen to show the structural properties of GaN surfaces under conventional growth conditions (i.e., high temperature).[33,50] Here, we are more interested in the low-temperature growth, where NH_3 + $3NH_2$ is most favored when using ammonia as N precursor.[52] On the other hand, we find that if N_2H_4 is used as the N precursor it is readily decomposed to NH_2, which indicates that the most stable surface should be NH_2 rich for the low temperature growth conditions.

In addition to the effects described under conventional experimental growth condition, recent DFT studies also show that the adsorption energy on the GaN (0001) surface depends on the position of the Fermi level because of possible charged surface states.[53−55] Specifically, the adsorption energy is not affected if there is no charge transfer process, whereas the adsorption energy depends on the energy of the surface state pinning Fermi level at the surface when there charge transfer occurs. For the nonpinned Fermi level at the surface, the adsorption energy depends on the bulk doping in the bulk.[54] It would be interesting, but beyond the scope of this article, to examine how this affects the growth process when using N_2H_4 as the N precursor.

Recently, Kempisty et al. reconstructed the phase diagram of GaN(0001) surface in an ammonia environment considering the possible charged surface states.[55] In particular, they divided the configuration space into three zones of differently pinned Fermi levels: at the Ga broken bond state for dominantly bare surface (region I), at the valence band maximum (VBM) for the NH_2 and H-covered surface (region II), and at the conduction band minimum (CBM) for the NH_3-covered surface (region III). Our study examines the bare Ga surface conditions (i.e., analogous to region I in the work from Kempisty and co-workers). It would also be interesting to study the surface state effects for the N_2H_4 molecule for an NH_2 covered surface, and this will be considered for a future publication.

III-2. Gallium Species on the N Rich Surface. *III-2-1. GaN (0001) Nitrogen Surface Model.* To examine the Ga layer growth, we consider TMG and TEG as the gallium

DOI: 10.1021/jp5116405
J. Phys. Chem. C XXXX, XXX, XXX−XXX

precursors. The larger size of these precursors required a larger surface model, and hence, we rotated the hexagonal lattice and made "a" along $(2\bar{1}\bar{3}0)$ direction, "b" along $(01\bar{1}0)$ direction, which led to a (0001) surface with 8 Ga sites for each double layer. The surface structure during GaN growth can be very complex and highly dependent on the experimental temperature growth conditions.[52] To simplify our simulation model, without sacrificing chemical accuracy, we focus on exploring the low energy reconstructed surfaces that satisfy the ECR at T = 0 conditions. These structures correspond to the temperature lower-bound geometries for GaN growth.[52] Because each surface Ga is partially filled with 3/4 of an electron, the surface has a total of 6 electrons. The growth nitrogen layer should balance these 6 surface electrons based on the Electron Counting Rule (ECR). Thus, any combinations of N species with 6 electrons could grow on this gallium layer, for example, $6NH_2$, 3NH, or 2N. Based on the above surface binding energy calculation, the lowest surface energy will be NH or N on the H3 site. However, only two N would fit on the surface for a total binding energy of −254.83 kcal/mol compared to having $6NH_2$ with a total binding energy of −498.58 kcal/mol. Consequently, we chose the lowest energy surface for an N layer to have $6NH_2$ adsorbed species. This surface was annealed at 600 K within 4 ps in quantum molecular dynamics, and minimized in energy, which led to 4 NH_2 on T1 sites and $2NH_2$ on Br sites as shown in Figure 5. The next section discusses the

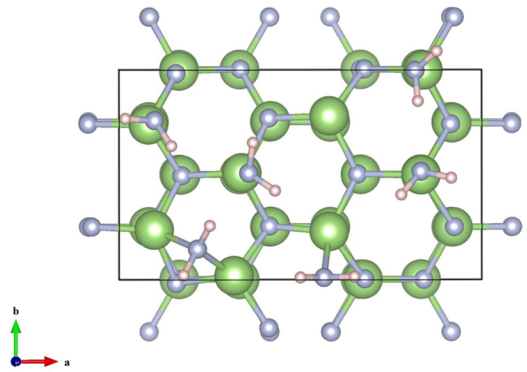

Figure 5. Simulation model of GaN (0001) surface with $6NH_2$ species (the top view). This model is used to examine the TMG surface reactions.

TMG reactions on this $6NH_2$ surface. Van de Walle and Neugebauer[50] define the lowest chemical potential N surface for GaN(0001) to be $6NH_2 + 2NH_3$. We assume for an ALD or CVD GaN growth process that H will be abstracted, via H radicals, from NH_3 to form NH_2. If this occurs for the $6NH_2 + 2NH_3$ surface, the decomposition route must satisfy the electron counting rule (ECR). We chose $6NH_2$ because it corresponds to the minimum energy system that maximizes the number of low coordination N, while satisfying the ECR. This is the most likely surface when using N_2H_4 as N precursor.

III-2-2. TMG Growth Mechanism. The TMG surface reaction mechanism on NH_2 sites of a GaN (0001) surface is shown in Figure 6, and the reaction barriers and heat of reactions are listed in Table 4. Initially, the TMG molecule is physical absorbed on the top of an NH_2 (T1 site, shown in Figure 6a) with heat of reaction of −5.51 kcal/mol. The distance between the TMG Ga and the surface N in NH_2 is 2.272 Å, which is 14% longer than the crystal Ga−N bond

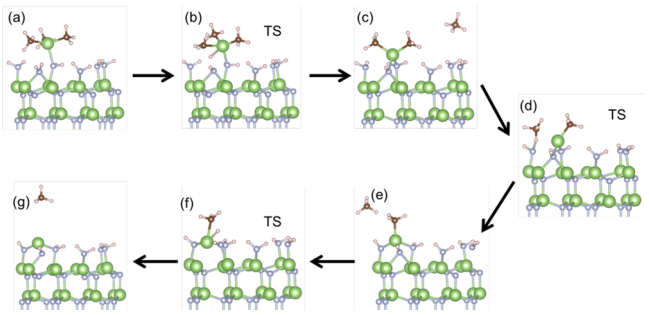

Figure 6. TMG decomposition reactions pathways on the N rich Ga (0001) surface. (a) is the initial state with TMG on surface, (b) (d) (f) are transition states, (c) is the intermediate state with DMG on surface, (e) is the intermediate state with MMG on surface. The CH_4 will be removed in the next step as it forms and is released to gas phase.

Table 4. TMG Surface Reactions (Unit: kcal/mol) on $6NH_2$ Bonded Ga (0001) Surface[a]

reactions	reaction barrier	heat of reaction
TMG(S) => DMG(S) + CH_4(G)	29.50	−23.49
DMG(S) => MMG(S) + CH_4(G)	42.54	−2.3
MMG(S) + H(G) => Ga(S) + CH_4(G)	29.70	−7.91

[a](S) represents the surface states, and (G) represents the gas phase states.

(1.992 Å). This indicates a weak interaction of the N lone pair with the empty orbital of Ga as TMG physically absorbs on the NH_2.

Then, one CH_3 reacts with a H from a bridged NH_2 to release one CH_4 from surface with reaction barrier of 29.5 kcal/mol and a heat of reaction of −23.49 kcal/mol. In the corresponding transition state, shown in Figure 6b, the N−H bond in NH_2 stretches from 1.026 to 1.508 Å. Meanwhile, the Ga−C bond is stretched from 2.035 to 2.296 Å, and the distance between C and H decreases from 2.643 to 1.302 Å. The TMG is then chemical adsorbed on the surface NH_2 because the Ga−N bond decreases from 2.272 to 2.058 Å. After this occurs, a dimethylgallium (DMG) forms on the N-rich surface, connected to one NH_2 on T1 site and one NH on Br site, as shown in Figure 6c.

It then follows that one CH_3 from the DMG reacts with the H on NH_2 (T1 site) to form another CH_4 with a reaction barrier of 42.54 kcal/mol and a heat of reaction of −2.3 kcal/mol. In the corresponding transition state, shown in Figure 6d, the N−H bond in NH_2 stretches from 1.026 to 1.577 Å, the Ga−C bond increases from 2.024 to 2.370 Å, and the C−H bond decreases from 2.480 to 1.268 Å. Another CH_4 is released into the gas phase and a monomethylgallium (MMG) forms on a T4 site, bonded to three surface nitrogen atoms, as shown in Figure 6e. We note that this T4 site corresponds to the precise Ga layer growth site and that no diffusion is necessary for the Ga layer growth under this mechanism.

The H source for the methyl abscission reaction in the previous steps comes from the surface N species. The last CH_3 from the MMG is too far from the surface H to react and release a final methane group. Thus, a gas phase H is needed to abstract the CH_3 and form CH_4, resulting in a bare surface Ga. This reaction has a reaction barrier of 29.70 kcal/mol, which is similar to the cost of TMG decomposing on a surface into DMG. At the corresponding transition state, shown in Figure

DOI: 10.1021/jp5116405
J. Phys. Chem. C XXXX, XXX, XXX−XXX

6f, the distance between C and a gas phase H needs to be 1.376 Å, and the distance between Ga and a gas phase H should be 1.902 Å. The final snapshot after this reaction is shown in Figure 6g.

The highest reaction barrier in this TMG reaction growth is the decomposition of DMG to MMG with an energy barrier of 42.54 kcal/mol. This means that an additional source of nonthermal energy is needed to grow crystalline GaN at low substrate temperatures (e.g., ultrashort laser pulses, shaped optical laser pulses, low-energy electron beams, among other options).

III-2-3. TEG Growth Mechanism. Triethylgallium (TEG) had also been experimentally used in the GaN and GaAs growth.[56,57] The grown GaN layers using triethylgallium as a precursor exhibited superior electrical and optical properties and a lower carbon impurity concentration.[56] This led us to study the reaction mechanism of TEG in the GaN growth process. We find that there are two possible reaction mechanisms for TEG in growing GaN: (1) beta hydride elimination (C_2H_4+H) and (2) direct desorption of C_2H_5 (similar to the TMG growth mechanism).[57] The calculated reaction barrier of direct desorption of the first C_2H_5 on the electron-balanced NH_2 rich surface is 27.3 kcal/mol. This is similar to direct desorption of CH_3 of TMG as showed above. For simplicity, we assume that the reaction mechanism and barrier for desorption of C_2H_5 is comparable to the CH_3 desorption when using TMG for GaN growth. Hence, we focus on the beta hydride elimination reactions and compare them with the TMG reactions reported above. We examined the beta-hydride elimination from a finite gas phase cluster using ab initio QM because we believe the electron balanced NH_2 surface may not involve this reaction.

The three steps for beta hydride elimination of TEG are shown in Table 5 including the reaction barrier and heat of reaction. The first C_2H_4 dissociation reaction has a reaction barrier of 30.0 kcal/mol with the heat of reaction of 26.10 kcal/mol. This reaction has a similar energy barrier as CH_4 dissociation from TMG on a Ga surface. This indicates that for TEG, both C_2H_4 formation by beta-hydride elimination and by direct desorption of C_2H_5 may happen in the growth process, which is consistent with existing experimental observations.[51] The second C_2H_4 dissociation reaction from diethylgallium (DEG) has a much higher reaction barrier of 55.12 kcal/mol, with a heat of reaction of 25.85 kcal/mol. The third C_2H_4 dissociation reaction from monoethylgallium (MEG), has an even higher barrier of 80.03 kcal/mol with a heat of reaction of 26.69 kcal/mol. The high-energy barrier C_2H_4 release reaction from DEG and MEG on this particular N-rich surface does not bluntly favor the use of TEG over TMG for GaN growth at low substrate temperatures. Nonetheless, experimental observations seem to suggest that the beat-hydride elimination reactions may be promoted (i.e., lower barriers) by increasing the Ga coverage on the surface[51] and that TEG leads to a reduction in the number of carbon impurities and defects. Studying the benefits of using TEG as precursor, instead of TMG, for defect-reduction in GaN growth is beyond the scope of this paper.

Table 5. TEG Beta-Hydride Elimination Reactions (Unit: kcal/mol) in Gas Phase Using PBE Functional

reactions	reaction barrier	heat of reaction
$GaEt_3$=>$GaEt_2$ + C_2H_4	30.00	26.10
$GaHEt_2$=>GaH_2Et + C_2H_4	55.12	25.85
GaH_2Et=>GaH_3 + C_2H_4	80.03	26.69

IV. SUMMARY

We have examined the reaction mechanisms involved in GaN growth with different nitrogen and gallium precursor molecules, including NH_3, N_2H_4, TMG, and TEG using ab initio QM calculations. We report on the binding energies, reaction barriers, and transition states of N_2H_4 and NH_3 decomposition on Ga (0001) surfaces, as well as on the effects of hydrogen transfer from the nearby species on the decomposition kinetics. We find that N_2H_4 has larger binding energy than NH_3 (~6 kcal/mol) to Ga, hence it is likely to happen at lower substrate temperatures, and that it offers a higher N yield for on a Ga-rich surface. We also find that initial NH_3 and N_2H_4 dissociation into NH_2 can proceed at low substrate temperatures (<100 °C) thanks to a low energy barrier (13.61 and 1.15 kcal/mol, respectively) and that further NH_2 decomposition to NH and eventually to N is favored by the hydrogen transfer from near neighboring N species on the surface. Nonetheless, NH_2 decomposition to NH and NH to N is likely to require additional input energy. Overall, we contend that the mobility of N species on a Ga (0001) surface may proceed, for the most part, at low substrate temperatures (<100C) and that the deposition of nitrogen layers in GaN is a reaction-limited process under low surface coverage conditions. For the gallium precursors, we find that the abstraction of secondary CH_3 groups through surface H from TMG is the rate-limiting process in GaN growth with this precursor (with a barrier of 42.54 kcal/mol) and that beta-hydrate elimination for TEG on N-rich surfaces has comparable energy barriers to the reactions of CH_3 desorption during TMG adsorption. Notwithstanding, we contend that due to the beta-hydride elimination, TEG favors growth with reduced C impurities over TMG.

AUTHOR INFORMATION

Corresponding Authors

*E-mail: ajaramil@caltech.edu. Tel.: 626-395-3591.
*E-mail: wag@wag.caltech.edu. Tel.: 626-395-2731.

Notes

The authors declare no competing financial interest.

ACKNOWLEDGMENTS

The authors would like to thank Prof. Steve George from the University of Colorado at Boulder for useful discussions concerning GaN growth using ALD. This work was partially funded by the Defense Advanced Research Projects Agency (DARPA) (Grant No. N660011214037, Drs. Tyler McQuade and Anne Fischer).

REFERENCES

(1) Parikh, R. P.; Adomaitis, R. A. An Overview of Gallium Nitride Growth Chemistry and its Effect on Reactor Design: Application to a Planetary Radial-Flow CVD System. *J. Cryst. Growth* **2006**, *286*, 259–278.

(2) Bandic, Z. Z.; Piquette, E. C.; Bridger, P. M.; Beach, R. A.; Kuech, T. F.; Mcgill, T. C. Nitride Based High Power Devices: Design and Fabrication Issues. *Solid-State Electron.* **1998**, *42*, 2289–2294.

(3) Maruska, H. P.; Tietjen, J. J. The Preparation and Properties of Vapordeposited Single Crystalline GaN. *Appl. Phys. Lett.* **1969**, *15*, 327–329.

DOI: 10.1021/jp5116405
J. Phys. Chem. C XXXX, XXX, XXX–XXX

(4) Nakamura, S.; Mukai, T.; Senoh, M. Candela-Class High-Brightness InGaN/AlGaN Double-Heterostructure Blue-Light-Emitting Diodes. *Appl. Phys. Lett.* **1994**, *64*, 1687−1689.
(5) Ponce, F. A.; Bour, D. P. Nitride-Based Semiconductors for Blue and Green Light-Emitting Devices. *Nature* **1997**, *386*, 351−359.
(6) Morkoc, H.; Strite, S.; Gap, G. B.; Lin, M. E.; Sverdlov, B.; Burns, M. Large-Band-Gap SiC, III-V Nitride, and II-VI ZnSe-Based Semiconductor Device Technologies. *J. Appl. Phys.* **1994**, *76*, 1363−1398.
(7) Orton, J. W.; Foxon, C. Group III-Nitride Semiconductors for Short Wavelength Light Emitting Devices. *Rep. Prog. Phys.* **1998**, *61*, 1−75.
(8) Kim, H. M.; Cho, Y. H.; Lee, H.; Kim, S. I.; Ryu, S. R.; Kim, D. Y.; Kang, T. W.; Chung, K. S. High-Brightness Light Emitting Diodes Using Dislocation-Free Indium Gallium Nitride/Gallium Nitride Multi-quantum Well Nanorod Arrays. *Nano Lett.* **2004**, *4*, 1059−1064.
(9) Pearton, S. J.; Zolper, J. C.; Shul, R. J.; Ren, F. GaN: Processing, Defects, and Devices. *J. Appl. Phys.* **1999**, *86*, 1−78.
(10) Strite, S.; Morkoc, H. GaN, AlN, and InN: A review. *J. Vac. Sci. Technol., B: Microelectron. Nanometer Struct.–Process., Meas., Phenom.* **1992**, *10*, 1237−1266.
(11) Burk, A. A., Jr.; O'Loughlin, M. J.; Siergiej, R. R.; Agarwal, A. K.; Sriram, S.; Clarke, R. C.; MacMillan, M. F.; Balakrishna, V.; Brandt, C. D. SiC and GaN Wide Bandgap Semiconductor Materials and Devices. *Solid-State Electron.* **1999**, *43*, 1459−1464.
(12) Wang, K.; Pavlidis, D.; Singh, J. Initial Stages of GaN/GaAs(100) Growth by Metalorganic Chemical Vapor Deposition. *J. Appl. Phys.* **1996**, *80*, 1823−1829.
(13) Motoki, K.; Okahisa, T.; Nakahata, S.; Matsumoto, N.; Kimura, H.; Kasai, H.; Takemoto, H.; Uematsu, K.; Ueno, M.; Kumagai, Y.; et al. Growth and Characterization of Freestanding GaN Substrates. *J. Cryst. Growth* **2002**, *237*−*239*, 912−921.
(14) Kuznia, J. N.; Khan, M. A.; Olson, D. T.; Kaplan, R.; Freitas, J. Influence of Buffer Layers on the Deposition of High Quality Single Crystal GaN over Sapphire Substrates. *J. Appl. Phys.* **1993**, *73*, 4700−4702.
(15) Koide, Y.; Itoh, N.; Itoh, K.; Sawaki, N.; Akasaki, I. Effect of AlN Buffer Layer on AlGaN/α-Al2O3 Heteroepitaxial Growth by Metal-organic Vapor Phase Epitaxy. *Jpn. J. Appl. Phys.* **1988**, *27*, 1156−1161.
(16) Doverspike, K.; Rowland, L. B.; Gaskill, D. K.; Freitas, J. A., Jr. The Effect of GaN and ain Buffer Layers on GaN Film Properties Grown on both C-Plane and A-Plane Sapphire. *J. Electron. Mater.* **1995**, *24*, 269−273.
(17) Theodoropoulos, C.; Mountziaris, T. J.; Moffat, H. K.; Han, J. Design of Gas Inlets for the Growth of Gallium Nitride by Metalorganic Vapor Phase Epitaxy. *J. Cryst. Growth* **2001**, *217*, 65−81.
(18) Okumura, H.; Misawa, S.; Yoshida, S. Epitaxial Growth of Cubic and Hexagonal GaN on GaAs by Gas-Source Molecular-Beam Epitaxy. *Appl. Phys. Lett.* **1991**, *59*, 1058−1060.
(19) Ross, J.; Rubin, M.; Gustafson, T. K. Single Crystal Wurtzite GaN on (111) GaAs with AlN Buffer Layers Grown by Reactive Magnetron Sputter Deposition. *J. Mater. Res.* **1993**, *8*, 2613−2616.
(20) Halpern, B. L.; Schmitt, J. J. Multiple Jets and Moving Substrates: Jet Vapor Deposition of Multicomponent Thin Films. *J. Vac. Sci. Technol., A* **1994**, *12*, 1623−1627.
(21) Ferguson, B. A.; Sellidj, A.; Doris, B. B.; Mullins, C. B. Supersonic-Jet-Assisted Growth of GaN and GaAs Films. *J. Vac. Sci. Technol., A* **1996**, *14*, 825−830.
(22) Guo, Q. X.; Okada, A.; Kindera, H.; Tanaka, T.; Nishio, M.; Ogawa, H. Heteroepitaxial Growth of Gallium Nitride on (1 1 1)GaAs Substrates by Radio Frequency Magnetron Sputtering. *J. Cryst. Growth* **2002**, *237*−*239*, 1079−1083.
(23) Tong, X. L.; Zheng, Q. G.; Hu, S. L.; Qin, Y. X.; Ding, Z. H. Structural Characterization and Optoelectronic Properties of GaN Thin Films on Si(111) Substrates using Pulsed Laser Deposition Assisted by Gas Discharge. *Appl. Phys. A: Mater. Sci. Process.* **2004**, *79*, 1959−1963.
(24) Sengupta, D.; Mazumder, S.; Kuykendall, W.; Lowry, S. A. Combined ab initio Quantum Chemistry and Computational Fluid Dynamics Calculations for Prediction of Gallium Nitride Growth. *J. Cryst. Growth* **2005**, *279*, 369−382.
(25) Fu, K.; Fu, Y.; Han, P.; Zhang, Y.; Zhang, R. Kinetic Monte Carlo Study of Metal Organic Chemical Vapor Deposition Growth Dynamics of GaN Thin Film at Microscopic Level. *J. Appl. Phys.* **2008**, *103*, 103524.
(26) Rapcewicz, K.; Nardelli, M. B.; Bernholz, J. Theory of Surface Morphology of Wurtzite GaN (0001) Surfaces. *Phys. Rev. B* **1997**, *56*, 12725−12728.
(27) Fritsch, J.; Sankey, O. F.; Smith, K. E.; Page, J. B. Ab initio Calculation of the Stoichiometry and Structure of the (0001) Surfaces of GaN and AlN. *Phys. Rev. B* **1998**, *57*, 15360−15371.
(28) Northrup, J. E.; Neugabauer, J. Indium-Induced Changes in GaN(0001) Surface Morphology. *Phys. Rev. B* **1999**, *60*, 8473−8476.
(29) Wang, F. H.; Kruger, P.; Pollman, J. Electronic Structure of 1 × 1 GaN(0001) and GaN(000 $\bar{1}$) Surfaces. *Phys. Rev. B* **2001**, *64*, 035305.
(30) Timon, V.; Brand, S.; Clark, S. J.; Gibson, M. C.; Abram, R. A. First-Principles Calculations of 2 × 2 Reconstructions of GaN(0001) Surfaces Involving N, Al, Ga, In, and As Atoms. *Phys. Rev. B* **2005**, *72*, 035327.
(31) Rosa, A. L.; Neugebauer, J. First-principles Calculations of the Structural and Electronic Properties of Clean GaN(0001) Surfaces. *Phys. Rev. B* **2006**, *73*, 205346.
(32) Elsner, J.; Haugk, M.; Jungnickel, G.; Frauenheim, Th. Theory of Ga, N and H Terminated GaN (0 0 0 1)/(0 0 0 $\bar{1}$) Surfaces. *Solid State Commun.* **1998**, *106*, 739−743.
(33) Van de Walle, C. G.; Neugabauer, J. Structure and Energetics of Nitride Surfaces under MOCVD Growth Conditions. *J. Cryst. Growth* **2003**, *248*, 8−13.
(34) Northrup, J. E.; Van de Walle, C. G. Indium versus Hydrogen-Terminated GaN(0001) Surfaces: Surfactant Effect of Indium in a Chemical Vapor Deposition Environment. *Appl. Phys. Lett.* **2004**, *84*, 4322−4324.
(35) Cardelino, B. H.; Cardelino, C. A. Dissociative Chemisorption of Trimethylgallium, Trimethylindium, and Ammonia on Gallium and Indium Nitride Substrates. A Computational Study. *J. Phys. Chem. C* **2011**, *115*, 9090−9104.
(36) Bermudez, V. M. Chemisorption of NH on GaN (0001) −(1 × 1). *Chem. Phys. Lett.* **2000**, *317*, 290−295.
(37) Timoshkin, A. Y.; Bettinger, H. F.; Schaefer, H. F., III DFT Modeling of Chemical Vapor Deposition of GaN from Organogallium Precursors: Thermodynamics of Elimination Reactions. *J. Phys. Chem. A* **2001**, *105*, 3240−3248.
(38) Kresse, G.; Hafner, J. Ab Initio Molecular Dynamics for Liquid Metals. *Phys. Rev. B* **1993**, *47*, 558−561.
(39) Kresse, G.; Furthmuller, J. Efficiency of Ab-Initio Total Energy Calculations for Metals and Semiconductors Using a Plane-Wave Basis Set. *Comput. Mater. Sci.* **1996**, *6*, 15−50.
(40) Kresse, G.; Furthmüller, J. Efficient Iterative Schemes for Ab Initio Total-Energy Calculations Using a Plane-Wave Basis Set. *Phys. Rev. B* **1996**, *16*, 11169−11186.
(41) Kresse, G.; Joubert, D. From Ultrasoft Pseudopotentials to the Projector Augmented-Wave Method. *Phys. Rev. B* **1999**, *59*, 1758−1775.
(42) Bochevarov, A. D.; Harder, E.; Hughes, T. F.; Greenwood, J. R.; Braden, D. A.; Philipp, D. M.; Rinaldo, D.; Halls, M. D.; Zhang, J.; Friesner, R. A. Jaguar: A High-Performance Quantum Chemistry Software Program with Strengths in Life and Materials Sciences. *Int. J. Quantum Chem.* **2013**, *113*, 2110−2142.
(43) Henkelman, G.; Jónsson, H. Improved Tangent Estimate in the Nudged Elastic Band Method for Finding Minimum Energy Paths and Saddle Points. *J. Chem. Phys.* **2000**, *113*, 9978−9985.
(44) Heyden, A.; Bell, A. T.; Keil, F. J. Efficient Methods for Finding Transition States in Chemical Reactions: Comparison of Improved Dimer Method and Partitioned Rational Function Optimization Method. *J. Chem. Phys.* **2005**, *123*, 224101.
(45) Kempisty, P.; Strąk, P.; Krukowski, S. Ab Initio Determination of Atomic Structure and Energy of Surface States of Bare and

DOI: 10.1021/jp5116405
J. Phys. Chem. C XXXX, XXX, XXX−XXX

Hydrogen Covered GaN (0001) Surface — Existence of the Surface States Stark Effect (SSSE). *Surf. Sci.* **2011**, *605*, 695−713.
(46) Chen, Y.-W.; Kuo, J.-L. Density Functional Study of the First Wetting Layer on the GaN (0001) Surface. *J. Phys. Chem. C* **2013**, *117*, 8774−8783.
(47) Walkosz, W.; Zapol, P.; Stephenson, G. B. A DFT Study of Reaction Pathways of NH3 Decomposition on InN (0001) Surface. *J. Chem. Phys.* **2012**, *137*, 054708.
(48) Himmerlich, M.; Lymperakis, L.; Gutt, R.; Lorenz, P.; Neugebauer, J.; Krischok, S. GaN(0001) Surface States: Experimental and Theoretical Fingerprints to Identify Surface Reconstructions. *Phys. Rev. B* **2013**, *88*, 125304.
(49) Gaskill, D. K.; Bottka, N.; Lin, M. C. Growth of GaN Films using Trimethylgallium and Hydrazine. *Appl. Phys. Lett.* **1986**, *48*, 1449−1451.
(50) Deng, Z.; Lu, X.; Wen, Z.; Wei, S.; Liu, Y.; Fu, D.; Zhao, L.; Guo, W. Mechanistic Insight into the Hydrazine Decomposition on Rh(111): Effect of Reaction Intermediate on Catalytic Activity. *Phys. Chem. Chem. Phys.* **2013**, *15*, 16172−16182.
(51) Zhang, P. X.; Wang, Y. G.; Huang, Y. Q.; Zhang, T.; Wu, G. S.; Li, J. Density Functional Theory Investigations on the Catalytic Mechanisms of Hydrazine Decompositions on Ir(1 1 1). *Catal. Today* **2011**, *165*, 80−88.
(52) Van de Walle, C. G.; Neugabauer, J. First-Principles Surface Phase Diagram for Hydrogen on GaN Surfaces. *Phys. Rev. Lett.* **2002**, *88*, 066103.
(53) Krukowski, S.; Kempisty, P.; Strąk, P. Fermi Level Influence on the Adsorption at Semiconductor Surfaces—Ab Initio Simulations. *J. Appl. Phys.* **2013**, *114*, 063507.
(54) Krukowski, S.; Kempisty, P.; Strąk, P.; Sakowski, K. Fermi Level Pinning and the Charge Transfer Contribution to the Energy of Adsorption at Semiconducting Surfaces. *J. Appl. Phys.* **2014**, *115*, 043529.
(55) Kempisty, P.; Strąk, P. Adsorption of Ammonia at GaN(0001) Surface in the Mixed Ammonia/Hydrogen Ambient - a Summary of Ab Initio Data. *AIP Advances* **2014**, *4*, 117109.
(56) Saxler, A.; Walker, D.; Kung, P.; Zhang, X.; Razeghi, M.; Solomon, J.; Mitchel, W. C.; Vydyanath, H. R. Comparison of Trimethylgallium and Triethylgallium for the Growth of GaN. *Appl. Phys. Lett.* **1997**, *71*, 3272−3274.
(57) Buchan, N. I.; Yu, M. L. Beta-Hydride Elimination Reaction of Triethylgallium on GaAs(100) Surfaces. *Surf. Sci.* **1993**, *280*, 383−392.

DOI: 10.1021/jp5116405
J. Phys. Chem. C XXXX, XXX, XXX−XXX